Journal of Pharmaceutical Innovation (2026) 21:245
https://doi.org/10.1007/s12247-026-10499-w

RESEARCH

Supramolecular nanosystems for rutin topical application

Maddalena Sguizzato[1] · Francesca Ferrara[1] · Stefano Manfredini[2] · Markus Drechsler[3] · Anna Baldisserotto[2] · Rita Cortesi[1]

Received: 5 November 2025 / Accepted: 15 February 2026

Abstract

Purpose This study presents the development of supramolecular nanosystems for the topical administration of rutin (RU), focusing on β-cyclodextrin (Cy) complexes and their inclusion in liposomes (CyL) in a 4:1 molar ratio.

Methods The supramolecular nanosystems were obtained by the "thin film hydration" method, and characterized in terms of size, morphology, encapsulation efficiency, antioxidant activity and skin safety, by DLS, transmission electron microscopy, UV spectrometry, DPPH radical liberation assay and patch test, respectively. Rutin release kinetics was determined by Franz cell experiments.

Results The resulting CyL loaded with RU formed stable, homogeneous vesicular dispersions, maintaining color, size, and polydispersity over 30 days, with rutin content consistently above 90%. Antioxidant activity, assessed by FRAP and DPPH assays, was significantly enhanced when RU was encapsulated in Cy and delivered via liposomes. In vitro diffusion studies using Franz cells revealed that CyL formulations provided a controlled release profile for RU, characterized by an initial increase followed by a plateau, suggesting vesicle-mediated release modulation. To improve topical applicability, CyL and Cy formulations were gelled with carbopol or xanthan gum, resulting in pseudoplastic, non-Newtonian gels. Gels containing CyL exhibited reduced spreadability and increased adhesiveness, supporting effective skin application. Patch tests on healthy volunteers confirmed good skin tolerability of all formulations.

Conclusions These findings demonstrate that the combination of cyclodextrin complexation and liposomal encapsulation, followed by gelation, offers a promising dual strategy to enhance the topical delivery and antioxidant efficacy of rutin.

Keywords Skin barrier · Delivery/penetration · Formulation stability · Antioxidants · Cyclodextrin · Patch test

Introduction

The skin represents the main barrier against environmental harmful agents of different origins, but also one of the entry routes of toxic substances into the body [1, 2]. Therefore, it represents the most vulnerable target to anomalous exposure to external stressors such as ozone (O_3), air pollutants and ultraviolet (UV) light [3, 4]. The main mechanism underlying the damaging effect of environmental insults on the skin is the generation of oxidative stress that reduces its antioxidant capacity [3]. The alteration of the skin barrier function may be responsible for the onset of skin diseases, including erythema, edema, dermatitis, psoriasis, photoaging and cancer [3].

Currently, the use of naturally derived ingredients for the development of cosmetic and dermatological products is a prerogative for companies in the sector. Plants have always been considered the primary source of natural active substances that can be used in the health sector. Natural compounds have been shown to act as potent anti-cancer agents by triggering apoptosis and inhibiting tumor cell proliferation and metastasis [5]. In this context, polyphenolic compounds, and in particular flavonoids, play a significant role due to their important antioxidant and anti-inflammatory activity, after topical application. Among these, the flavonol

✉ Rita Cortesi
crt@unife.it

[1] Department of Chemical, Pharmaceutical and Agricultural Sciences (DoCPAS), Via Fossato di Mortara, 19, Ferrara I-44121, Italy

[2] Department of Life Sciences & Biotechnology, University of Ferrara, Ferrara, Italy

[3] Macromolecular Chemistry II, University of Bayreuth, Bayreuth, Germany

Published online: 04 March 2026

glycoside rutin (RU) is attracting considerable interest as a therapeutic agent in various pharmaceutical or cosmeceutical formulations [6, 7]. In particular, RU was found to be effective in counteracting skin lesions induced by environmental stressors [8, 9]. Furthermore, due to its structural similarity to organic UV filters and its strong antioxidant activity, RU has been shown to be effective against damage induced by UV radiation [9–11], providing an improvement in the sun protection factor (SPF) [12, 13]. In addition, RU can reduce skin photoaging by strengthening the density and elasticity of the skin [8, 14]. Recent studies have investigated the possible use of RU in the treatment of skin carcinomas, such as melanoma, even if they offer preliminary information on its pro-apoptotic effect in vitro on murine and human melanoma cells [15], leaving the antitumor effect still to be clarified.

However, one of the main drawbacks of RU is the poor solubility in water and bioavailability, so in recent decades, delivery systems have been widely studied [16, 17], with the aim of increasing the efficacy of the drug and also the contact time with the site of action, thus trying to improve its absorption and control the release [18–20]. Based on these considerations, the present study aims to design supramolecular systems for the delivery of RU, suitable for topical application. Given the difficulties of solubilizing RU, different systems are investigated and compared, namely cyclodextrins and liposomes. Precisely, in this study, β-cyclodextrin (Cy), is used and the inclusion complex containing rutin (Cy/RU) was incorporated in liposomal systems leading to the formation of liposomes loaded with rutin/β-cyclodextrin complex, RUCyL. This strategy leverages the improved solubility, stability, and bioavailability of the active ingredient in a formulation conferred by cyclodextrin complexation, alongside the vesicular structure of liposomes can incur a controlled release and prolonged stability of the drug. Furthermore, the present study also aims to evaluate the performance of the produced nanosystems, after increasing their viscosity by means of a pair of thickening agents, to improve their topical application.

Materials and Methods

Materials

Rutin (RU), hydroxypropyl-β-cyclodextrin (Cy), cholesterol (CH), phosphatidylcholine (PC), xanthan gum (XG) and carbopol (CRP) were from Sigma-Aldrich (St Louis, MO, USA). All other materials and solvents were from Merck Serono S.p.A. (Rome, Italy).

Preparation and Characterization of Cy/RU and RUCyL

The complexes of Cy and RU (Cy/RU) were prepared in water at the 4:1 molar ratio. Notably, after weighing Cy and RU using an analytical balance (ACCULAB, Sartorius AG, Göttingen, Germany), they were dispersed by swirling and sonication in an ultrasonic bath (Branson 2510, Cinisello Balsamo, Italy) for 15 min and left in an orbital shaker for 24 h [21].

RUCyL were prepared by the "thin film hydration" method followed by ultrasonication (Branson 2510, Cinisello Balsamo, Italy) [22]. Precisely, a mixture of PC and CH (4:1 mol/mol) in methylene chloride: methanol (1:1 v/v) was poured into a round-bottom flask and evaporated under reduced pressure conditions ($p \cong 60$ bar) in a Buchi Rotavapor R-200 (Cornaredo, Italy). The formed thin lipid film was then hydrated by swirling (VELP scientifica s.r.l., Usmate Velate, Italy) with the aqueous complex Cy/RU and ultrasonicated for 30 min in a Branson 2510 bath (Cinisello Balsamo, Milan, Italy).

The morphology of RUCyL was investigated using a Cryogenic Transmission Electron Microscope (Cryo-TEM) (Zeiss EM 922 Omega TEM, Gatan Inc., Pleasanton, CA, USA) equipped with a cryo holder CT3500 [23]. Specimens were visualized using doses of approximately 1000–2000 e/nm2 at 200 kV at a sample temperature of below − 175 °C, and the obtained images were recorded by a CCD camera and processed with GMS 1.4 software (Gatan Inc., Pleasanton, CA, USA).

RUCyL size measurements, performed on aqueous diluted fractions (1:10 by volume), were conducted with a Zetasizer Nano S90 (Malvern Instr., Malvern, UK) equipped with a 5 mW helium-neon laser with a wavelength output of 633 nm. Measurements, conducted at 25 °C, 90° angle and run time around 180 s [24], allowed the obtaining of a dimensional distribution graph, as well as the Z-Average and PdI values of the vesicular formulations [25].

Determination of Rutin Content

A UV-VIS-NIR Spectrometer Lambda 19 spectrophotometer (Perkin Elmer, Beaconsfield, UK) equipped with quartz cuvettes with an optical path of 1 cm, and the Windows-based software application UV WinLab (Perkin Elmer, Beaconsfield, UK) was employed to determine the content of RU in the produced formulations. Specifically, the external standard method was selected as the quantitative analytical determination. Therefore, the mean values of at least 3 samples of each scalar dilution of RU in ethanol, ranging from 40 µg/ml to 2.5 µg/ml, were used to obtain the calibration

curve. Each concentration was analyzed at wavelength λ_{max} = 360 nm (R^2 = 0.9999) [26].

The encapsulation efficiency (EE) in RUCyL, expressed as RU content, was determined one day after production on a 300 µl sample of the formulation obtained after ultracentrifugation conducted at 8000 rpm for 20 min on a Spectrafuge™ 24D Digital Microcentrifuge (Woodbridge, NJ, USA) by means of a Microcon centrifugal filter unit YM-10 membrane (NMWCO 10 kDa, Sigma-Aldrich, St. Louis, MO, USA). 100 µl of the retentate ultracentrifuged sample was diluted with methanol (1:10, v/v) and subjected to magnetic stirring for 30 min before UV quantification of RU. The encapsulation parameter was calculated using Eq. (1).

$$EE = RU/T_{RU} \times 100 \quad (1)$$

where RU is the amount of rutin determined by UV, and T_{RU} is the total RU amount weighed to prepare the formulation. The RU estimation was carried out as described above using the calibration curve as a reference.

In Vitro Diffusion Experiments

RU diffusion was evaluated using Franz cells associated with a nylon membrane. Briefly, membranes were hydrated in distilled water at room temperature for 1 h before mounting on Franz diffusion cells (LGA, Berkeley, CA) with a 1 cm diameter orifice (0.78 cm^2 exposition area). The receiving phase, consisting of PBS 73mM (5 ml) at pH 7.4, was magnetically stirred at 300 rpm and maintained at 32 ± 1 °C during the experiments [27]. 1 ml of each formulation was poured in contact with the membrane surface in the donor chamber and 300 µl of the receiving phase were withdrawn at predetermined time points for RU content UV analysis. The removed receiving phase volume was replaced with an equivalent amount of PBS. The estimated mean values ± standard deviations of diffused RU, measured in four different experiments, were expressed as µg/cm^2 and plotted as a function of time.

The kinetic parameters were determined by linear regression analysis of the in vitro diffusion experimental data according to the best mathematical models expressing the kinetic release profile, namely zero-order (cumulative amount of drug released over time), first order (logarithmic cumulative amount of drug remained over time), Higuchi (cumulative amount of drug released over the square root of time) and Korsmeyer-Peppas equations (logarithmic fractional drug released over logarithm of time). The regression coefficient (R^2) and the release exponent (n) were determined, allowing the prediction of the mathematical model.

Antioxidant Activity

To rapidly assess the antioxidant capacity, the DPPH radical liberation assay [28] was used. This assay estimates the hydrogen-donating capacity of an antioxidant to convert the stable free radical DPPH into 1,1-diphenyl-2-picrylhydrazyl, which is accompanied by a deep purple to light yellow colorimetric reaction, which can be assessed by measuring the percentage reduction in absorbance of the solution at 517 nm after the reaction of the radical with the test products. The percentage scavenging capacity of the radical was obtained by applying Eq. (2), as follows:

$$DPPH\ radical\ scavenging\ capacity\ (\%) = [1 - (A1/A0)] \times 100 \quad (2)$$

where A0 is the absorbance of the control (without the antioxidant molecule, AM), and A1 is the absorbance in the presence of AM. AM (both in solution and in cyclodextrins) at different concentrations (0.750 mL) was added to a methanol solution of DPPH (1.5 mL). The absorbance at 517 nm was obtained with a UV-Vis spectrophotometer (ONDA UV-31 SCAN Spectrophotometer) as previously described [29]. The IC_{50} values obtained (µg/mL) were derived from calibration straight lines and are the mean ± standard deviation of at least three independent experiments.

The quantitative FRAP assay measures the plasma ferric ion-reducing capacity, as it is based on the reduction of ferric ions (Fe^{3+}) to ferrous ions (Fe^{2+}) under acidic conditions in the presence of 2,4,6-tripyridyl-s-triazine (TPTZ) [30]. Indeed, the presence of an AM allows the reduction of the Fe^{3+}–TPTZ complex to the ferrous form, resulting in an intense blue coloration measured at 593 nm (absorption maximum wavelength). Trolox was employed to perform the calibration curves; therefore, the FRAP antioxidant activity is given as µmol Trolox equivalent/g of compounds.

Gel Preparation and Characterization

To obtain thickened formulations, XG and CRP were added to the selected RU-containing Cy and CyL formulations. In particular, XG (0.5%, w/w) was added to the formulation, then manually mixed and planetary stirred overnight to achieve complete dispersion [31]. On the other hand, CRP (0.5%, w/w) viscosified formulations were prepared by magnetic stirring at 50 °C, planetary stirring overnight, followed by triethanolamine addition.

The viscosity of the thickened formulations was measured by means of a Brookfield, Helipath Stand rotational viscometer (Brookfield Engineering Laboratories, Massachusetts, USA). It is known that the determination of viscosity of a formulation depends on the properties of the system under examination, the type of viscometer, the impeller

used, the rotation speed, the temperature, the volume analyzed and the dimensions of the container. For the measure, 50 ml of gel were placed in a beaker and tested at a temperature of 25 °C. A cylindrical impeller was immersed inside, and the viscosity was measured at different speeds between 1 and 100 rpm [31].

The spreading capacity of gels was evaluated 24 h after gel preparation at 32 ± 1 °C [32]. Notably, 100 mg of the thickened formulation were poured on a 3 cm diameter Petri dish and pressed by means of a 10 g mass onto a glass dish. The time taken for the gel to completely fill the capsule was then evaluated. The spreadability test was repeated three times, and the mean values ± standard deviations were calculated using Eq. (3).

$$S = m \times 1/t \tag{3}$$

where S stands for gel spreadability, m for the weight (g) onto the dish top, l for the dish diameter (cm), and t for the time (s) taken by the gel to completely fill the dish diameter [32].

The in vitro leakage of gels was determined on rectangular agar slides obtained from dissolving agar (1.5% w/w) in citrate buffer (pH 5.5) followed by stirring at 95 °C until complete solubilization, cooling and cutting agar slides homogeneous in dimensions.

30 mg of gel were placed on one side of the agar slide inserted into a Petri dish positioned vertically at 90° and maintained at 32 ± 1 °C. After placing the gel on top of the slide, the time spent by the gel to flow down the slide was measured. Gel loss, expressed as the travel time of the gel on the plate, was repeated three times and the mean values ± standard deviations were determined.

Patch Test

To assess the effect of the produced formulations on intact human skin, an in vivo irritation test was conducted in agreement with the protocols for skin compatibility testing of potentially cutaneous irritant cosmetic ingredients on human volunteers [33–35]. Specifically, those volunteers suffering from dermatitis (a), skin allergic reactions (b) or undergoing treatment with all the types of anti-inflammatory drugs (a) were excluded from the study. 20 healthy volunteers of both sexes were subjected to an occlusive patch test after giving their written consent to the experiment. A Finn Chamber® (Bracco, Milano, Italy) made of aluminum and loaded with 10 mg of the formulation, was applied onto the forearm or back skin; then the skin was protected with self-adhesive tape. The formulations were left in contact with the skin for 48 h, then the patch was removed, and the skin was cleansed 15 min and 24 h after removal. Therefore, the irritative reactions were expressed as a percentage of the total number of reactions occurring in volunteers after assessing and classifying the erythematous and/or edematous reactions as mild, clearly visible, or moderate/severe erythema.

Statistical Analysis

GraphPad Prism 10 (Version 10.3.1 (464), GraphPad Software Inc., La Jolla, CA, USA) was used to perform the statistical analysis. For each of the variables tested, an analysis of variance (2-way ANOVA), followed by Tukey's post hoc test, was assessed. The data are expressed as the mean ± SD of triplicate determinations obtained in three independent experiments, and a p value < 0.05 was considered statistically significant.

Results and Discussion

Preparation and Characterization of Cy/RU and RUCyL

Cy/RU and RUCyL were prepared and characterized as described in the Materials and Methods section. Particularly, the complex Cy/RU (4:1 mol/mol) was prepared in water leading to a limpid, yellowish and transparent solution [21], whereas RUCyL supramolecular dispersion (25 mg/ml final content of lipids) was obtained by the "thin layer evaporation" method followed by sonication, leading to yellowish milky suspensions.

Morphological analysis of liposomes containing β-cyclodextrin (CyL) and RUCyL based on cryo-TEM, highlighted the prevalent presence of unilamellar vesicles not influenced in terms of size or lamellarity by the presence of rutin (Fig. 1); while regarding the dimensions and size distributions of CyL and RUCyL, the TEM images corroborates with the data obtained by photon correlation spectroscopy (PCS) indicating that the presence of RU induced an increase in both the vesicles size and the polydispersity index values (Table 1).

Drug Loading and Formulation Stability

The content of RU in the considered supramolecular systems, namely Cy and CyL was evaluated after production and over time up to 30 days after production.

Precisely, from data reported in Fig. 2 it is evident that the RU entrapment efficiency in both Cy/RU and RUCyL reaches 90% of the total amount of RU used for the preparations, which is comparable to values reported for similar cyclodextrin-based systems [20, 36, 37] and equivalent to

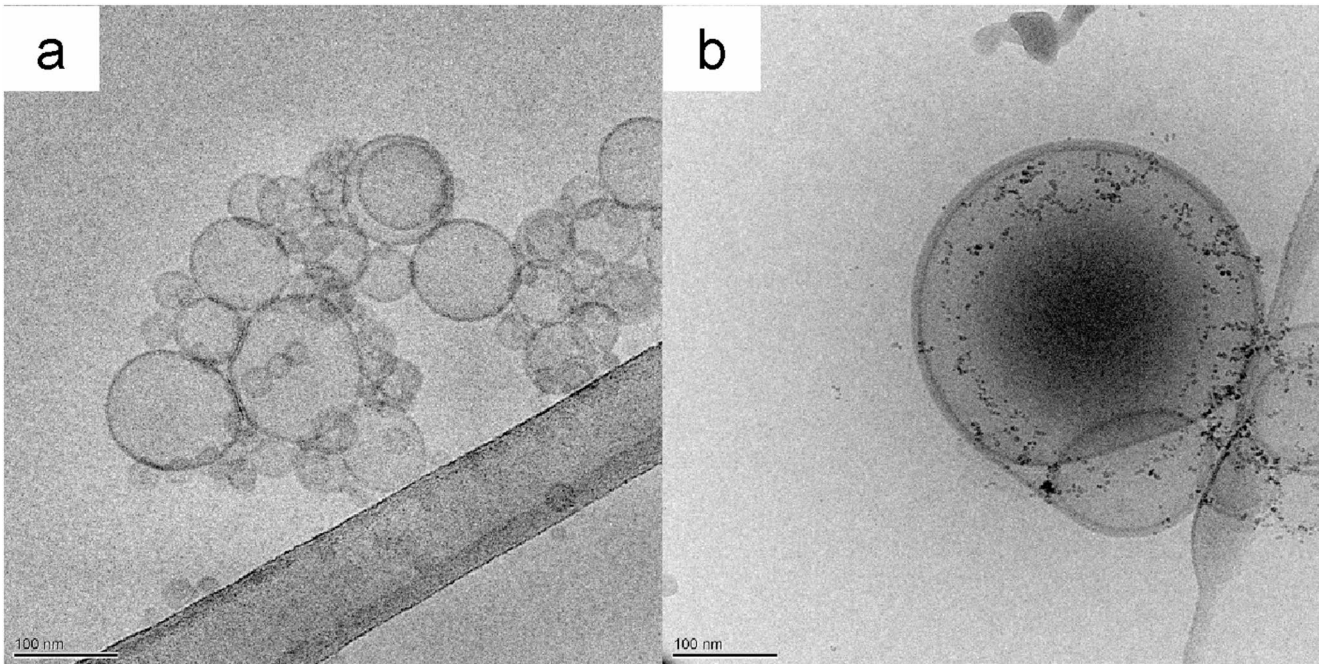

Fig. 1 Cryo-TEM images of CyL (**a**) and RUCyL (**b**). The bars represent 100 nm

Table 1 Dimensional parameters of CyL and RUCyL after production, expressed as Z-average (nm) and Polydispersity index. Data are the mean of 3 batches ± s.d

Formulation	Z-average (nm)	Polidispersity Index
CyL	349.23 ± 8.07	0.189 ± 0.08
RUCyL	427.76 ± 9.10	0.234 ± 0.07

or better than previously described vesicular formulations for polyphenols [38–40]. Nevertheless, after RUCyL centrifuged filtration, it is shown that RU is mainly associated (at least 65% of the total RU content) to the lipidic fraction of the supramolecular system CyL.

The stability of RU content within RUCyL showed the overtime maintenance of percentages higher than 95% (see Fig. 3).

Regarding the dimensional stability of the produced systems, verified on day 1, 14 and 30 days after preparation, it was evidenced that the size of RUCyL is almost stable over time, with a slight reduction of a few nanometers. On the other hand, PdI values (close to 0.2) indicated the presence of heterogeneous populations especially at day 1 and 14 (Fig. 3).

In Vitro Studies

Antioxidant Activity

The radical scavenging ability of the encapsulated RU has been evaluated after inclusion in Cy and CyL and compared to that of the corresponding amount of RU solubilized in ethanol, to assess the efficiency of the Cy-based systems and to preserve RU effect. Precisely, two different assays were employed in order to get information on the antioxidant activity in terms of both radical removal ("2,2-diphenyl-1-picrylhydrazyl, DPPH) and ferric-ion reduction power (FRAP). The first one allows for the measurements of the reducing activity of antioxidant molecules against the DPPH radical by a colorimetric reaction.

The IC_{50} DPPH values shown in Table 2 suggest that the antioxidant potential of RU was enhanced after complexation with Cy. Indeed, the IC_{50} values of RU in both Cy and CyL decreased in a statistically significant manner compared to RU in solution ($p = 0.0271$ and $p = 0.0057$ respectively). This increase in antioxidant activity of RU could be attributed to the improved solubility of the drug due to the delivery system.

Similarly, FRAP results showed increased activity in both Cy and CyL compared to the solution, with extreme and highly statistically significant changes, respectively ($p < 0.0001$ and $p = 0.0054$).

Therefore, the antioxidant activity, as measured by DPPH and FRAP assays, showed a statistically significant enhancement compared to RU in solution, in line with or exceeding results from similar delivery systems described in the literature [12, 41, 42].

When comparing the two formulations, Cy/RU and RUCyL, the DPPH assay revealed no statistically significant difference ($p = 0.0817$), indicating only a trend in favor of RUCyL. In contrast, the FRAP assay showed a marked difference between the two formulations, which was found

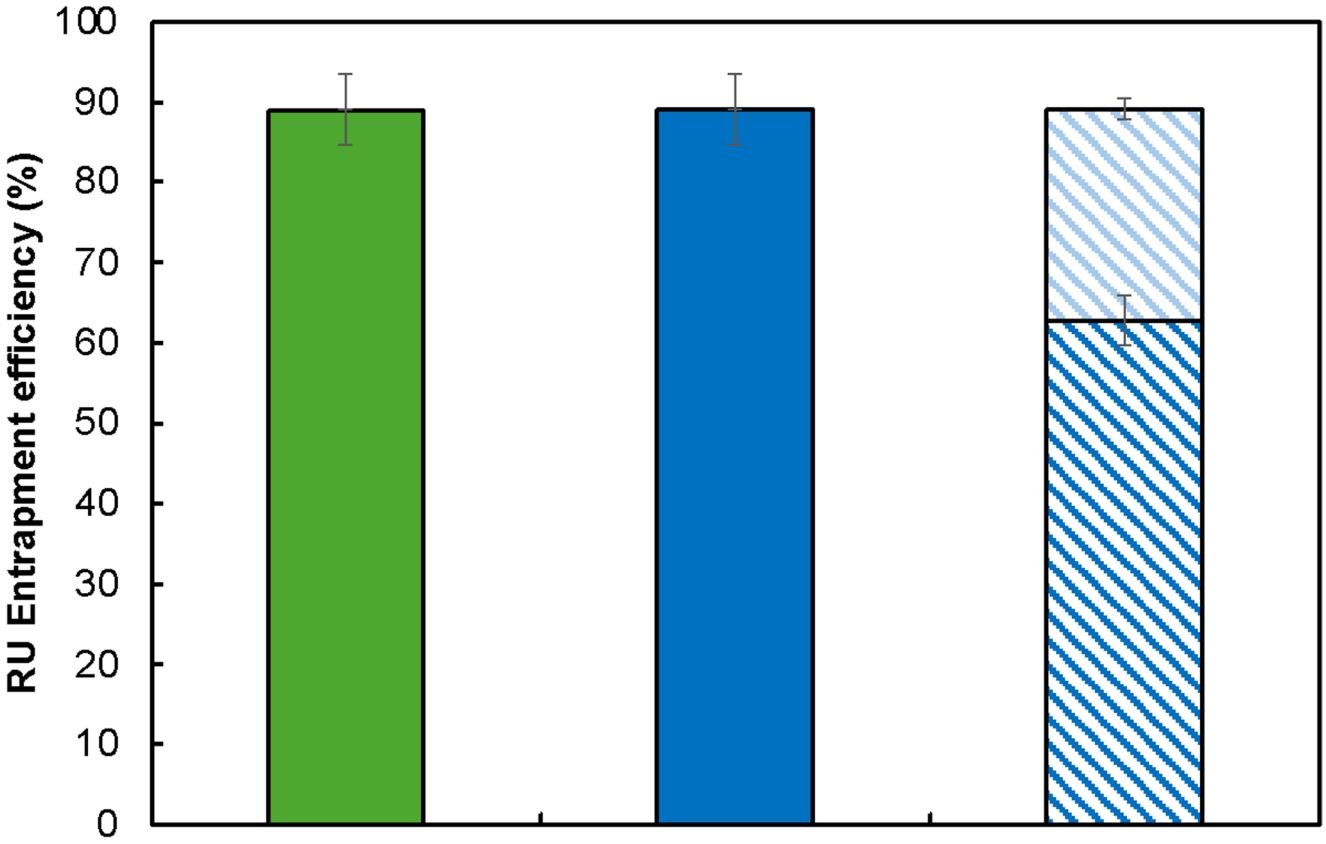

Fig. 2 RU entrapment efficiency in Cy/RU (green), RUCyL (blue), RUCyL lipid fraction (blue stripes) and RUCyL aqueous fraction (light-blue stripes) obtained after centrifugal filtration

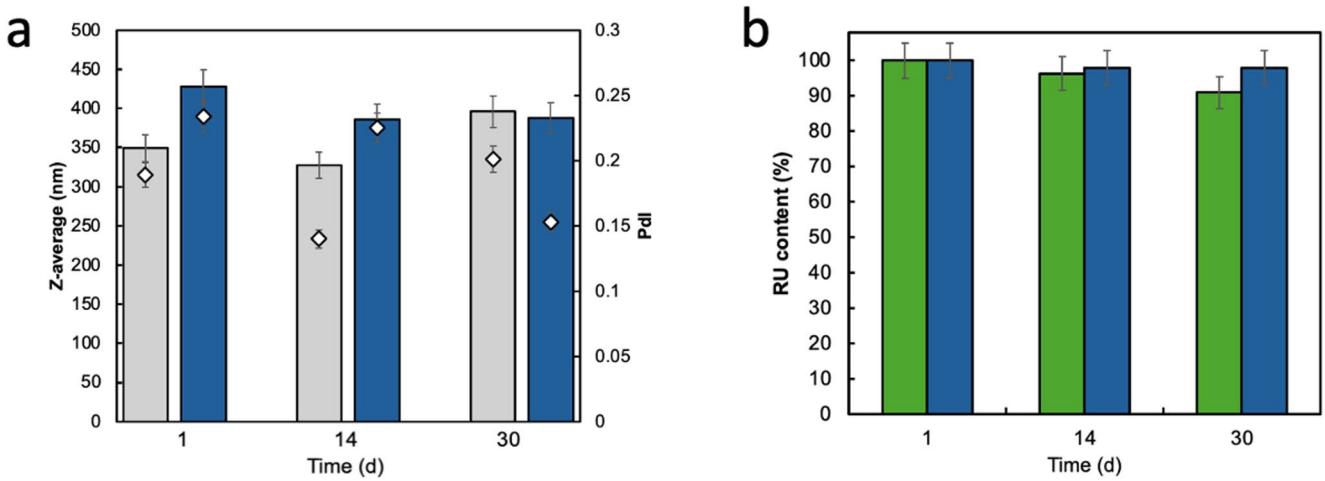

Fig. 3 Dimensional (**a**) and drug content (**b**) stability of RUCyL (blue) over time. Dimensional parameters are expressed as average diameter (histograms) and polydispersity index (diamonds). As a comparison, the dimensional stability of empty CyL (grey) (panel a) and the content of rutin within the Cy/RU complex (green) (panel b) during time are reported. Values are the mean of 3 batches ± s.d

to be very statistically significant ($p = 0.0075$), suggesting a higher reducing capacity of the Cy/RU system compared to RUCyL.

Indeed, the DPPH assay, which mainly reflects radical scavenging ability through hydrogen atom or electron transfer mechanisms, showed no statistically significant difference between the two formulations. Conversely, the FRAP assay, based exclusively on electron-transfer reactions and strongly influenced by the accessibility of redox-active groups, revealed a markedly higher reducing power

Table 2 Antioxidant activity of the produced formulations compared with ethanolic solution of Rutin, as determined by DPPH and FRAP assays

Formulation	DPPH IC_{50} (μg/ml) ± s.d.	FRAP μmol TE[1]/g ± s.d.
RU/EtOH	10.33 ± 0.98	2296.32 ± 110.97
Cy/RU	7.80 ± 0.63	3413.02 ± 175.23
RUCyL	6.70 ± 0.53	2754.67 ± 21.56

[1] TE = equivalent Trolox®

for Cy/RU. These results suggest that the different supramolecular organization of RU within Cy and CyL systems may differentially affect the availability of functional groups involved in electron donation, leading to assay-dependent antioxidant responses.

Viscosity, Spreadability and Leakage Behavior

The consistency of a formulation is an important property for topical application and viscosity plays a fundamental role in controlling the permeation of the applied drug. To confer to the Cy-containing formulations an adequate viscosity for cutaneous administration, xanthan gum (XG) and carbopol (CRP) were selected after a preliminary screening (data not shown) and added to the RU-containing Cy and CyL formulations as described in the Materials and Methods section. Specifically, XG was added to the formulation, then manually mixed and planetary stirred overnight to favor its complete dispersion [31]; CRP thickened formulations were prepared by magnetic and planetary stirring followed by addition of triethanolamine. Afterwards, a rotational viscometer was employed to measure the rheological behavior of the thickened formulations.

The viscosity curves of the different analyzed preparations (Fig. 4a), show a similar profile. In particular, the viscosity value varies with the velocity gradient indicating a typical non-Newtonian fluid behavior. Indeed, in all cases, the measure of the fluid's resistance to its flow (i.e., viscosity) decreases as the shear stress increases. This behavior, called "shear thinning", is typical of pseudoplastic fluids and characterizes gelled systems with polymers at certain concentrations.

Spreadability is also an important parameter for formulations intended for topical application as it influences patient compliance and certain technological aspects such as extrusion from the package and uniform application on the skin [31].

The spreadability test was conducted in triplicate on the thickened formulations, and the mean value and standard deviation were calculated (Fig. 4b). Fluid systems are known to exhibit high spreadability due to their rapid spreading time. From the analysis of results summarized in Fig. 4b, it is possible to observe that the spreadability value of thickened RUCyL is lower than thickened Cy/RU. Therefore, Cy/RU thickened formulations take less time to distribute to the application site, confirming the results obtained with the viscosity test.

The leakage test enables us to make some considerations about the ability of the gel to adhere to the skin surface. For the thickened systems, the test is performed in triplicate, and the results reported in Fig. 4c are the mean value ± standard deviation. In addition, the data are expressed in terms of the space occupied in 1 min of time. It is possible to observe that the Cy/RU system occupies a larger space of the plate, while the RUCyL system remains in situ for a longer time. This result agrees with the above described spreadability and viscosity data.

In Vitro Diffusion Experiments

The study on the diffusion of rutin was conducted using the Franz cells associated with a nylon membrane to evaluate the influence of the delivery system on the release of RU. The method is described in the Methods section, and phosphate buffer solution (PBS) 73mM pH 7.4 was used as the receiving phase.

Figure 5 shows the diffusion profile of RU from the produced formulations. The formulations in aqueous dispersion

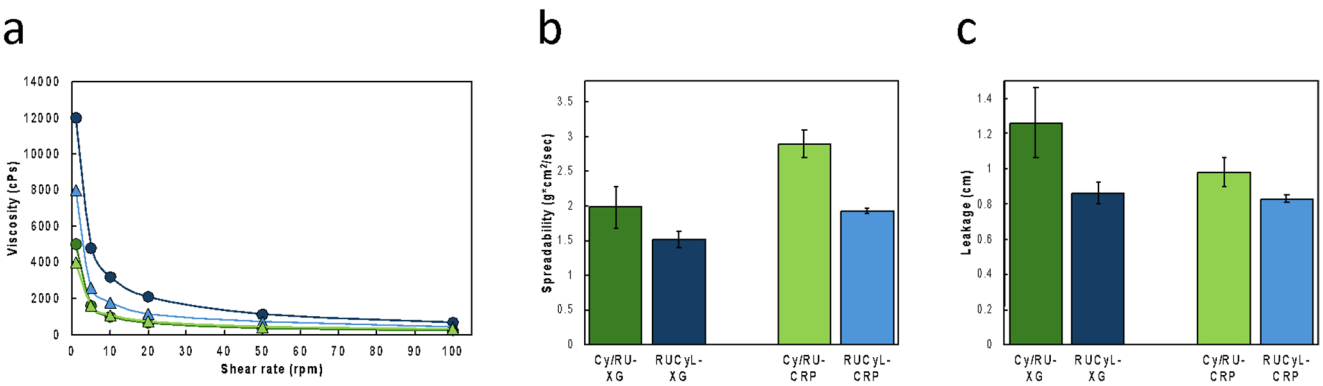

Fig. 4 Viscosity (**a**), spreadability (**b**) and leakage (**c**) characteristics of Cy/RU (green) and RUCyL (blue) after addition of xanthan gum (XG, dark color) and carbopol (CRP, light color) to the formulations

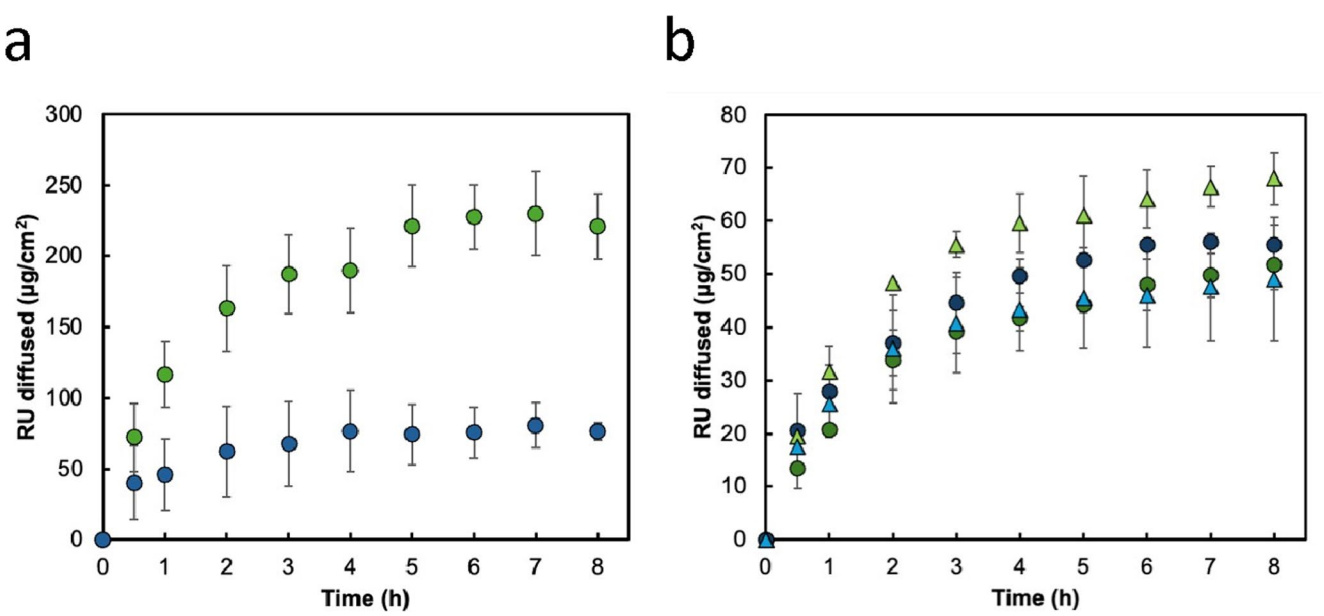

Fig. 5 In vitro release profiles of rutin from Cy/RU (green) and RUCyL (blue) in water dispersion (**a**) or in gel (**b**) namely xanthan gum (XG, circle) or carbopol (CRP, triangles). PBS was used as the receiving phase. Data are the mean of four unrelated experiments ± s.d., with Cy/RU vs. RUCyL, RUCyL vs. RUCyL-XG, RUCyL vs. RUCyL-CRP, Cy/RU vs. Cy/RU-XG, Cy/RU vs. Cy/RU-CRP, $p < 0.0001$ by 2-way ANOVA followed by Tukey's post hoc comparison test

(Fig. 5a) showed flux values, obtained by dividing the calculated concentration by the membrane area through which the drug diffuses (0.78 cm^2), significantly higher in the case of Cy/RU with respect to RUCyL. This result suggests that the inclusion of Cy/RU in liposomal formulation allows the controlled release of the drug over time ($p < 0.0001$). Moreover, the diffusion profiles of the formulations in aqueous dispersion resulted as significantly higher than those of the thickened systems ($p < 0.0001$), due to the viscosity of the system being inversely proportional to the release rate. Figure 5b highlights that the diffusion profiles of the two thickened RUCyL systems are similar and range from 49 to 55 µg/cm^2. This behavior could probably be due to the use of one polymer over another that does not influence the release of RU, which is instead controlled by the presence of vesicles. As regards the thickened complexes, the profile is different. The flux of Cy/RU-CRP is higher than that of Cy/RU-XG, probably due to the chemical structure of xanthan gum, or the sol-gel state of the polymer. It is known that each polymer has a characteristic transition temperature; in the sol state, the polymer chains are free and independent from each other and therefore they have a high mobility, while in the gel state they are more ordered and less free to move. Since this study was conducted at a temperature of 32 °C, this likely affected the sol/gel composition of the polymer, inducing a higher fraction of the sol state and consequently influencing the diffusion of rutin. Based on these considerations, further in-depth investigation is needed to identify the optimal viscosity agent to obtain a formulation intended for a most effective topical application.

Table 3 Kinetic parameters (R^2 and n values) of rutin diffused from the different formulations

Formulation	R^2			
	Zero-order	First-order	Higuchi	Korsmeyer-Peppas (n)
Cy/RU	0.8962	0.9300	0.9586	0.9667 *(0.46)*
Cy/RU-XG	0.8817	0.8869	0.9552	0.9701 *(0.53)*
Cy/RU-CRP	0.8622	0.8698	0.9443	0.9619 *(0.50)*
RUCyL	0.8861	0.8899	0.9482	0.9710 *(0.30)*
RUCyL-XG	0.9542	0.9584	0.9941	0.9983 *(0.41)*
RUCyL-CRP	0.8840	0.8892	0.9584	0.9759 *(0.42)*

To further evaluate which type of mechanism governs the rutin diffusion from the Cy complexes and liposomes in aqueous or thickened form, the released data obtained by Franz cells experiments were plotted into different mathematical models. The resulting values of R^2 reported in Table 3, reveals that all the formulations followed Korsmeyer-Peppas release kinetic model, suggesting the diffusion-based mechanism, quite similar to Higuchi profile, and the suitability of the formulations for transdermal effect. Moreover, in order to clarify process involved, the analysis of the release exponents, i.e. n values obtained by

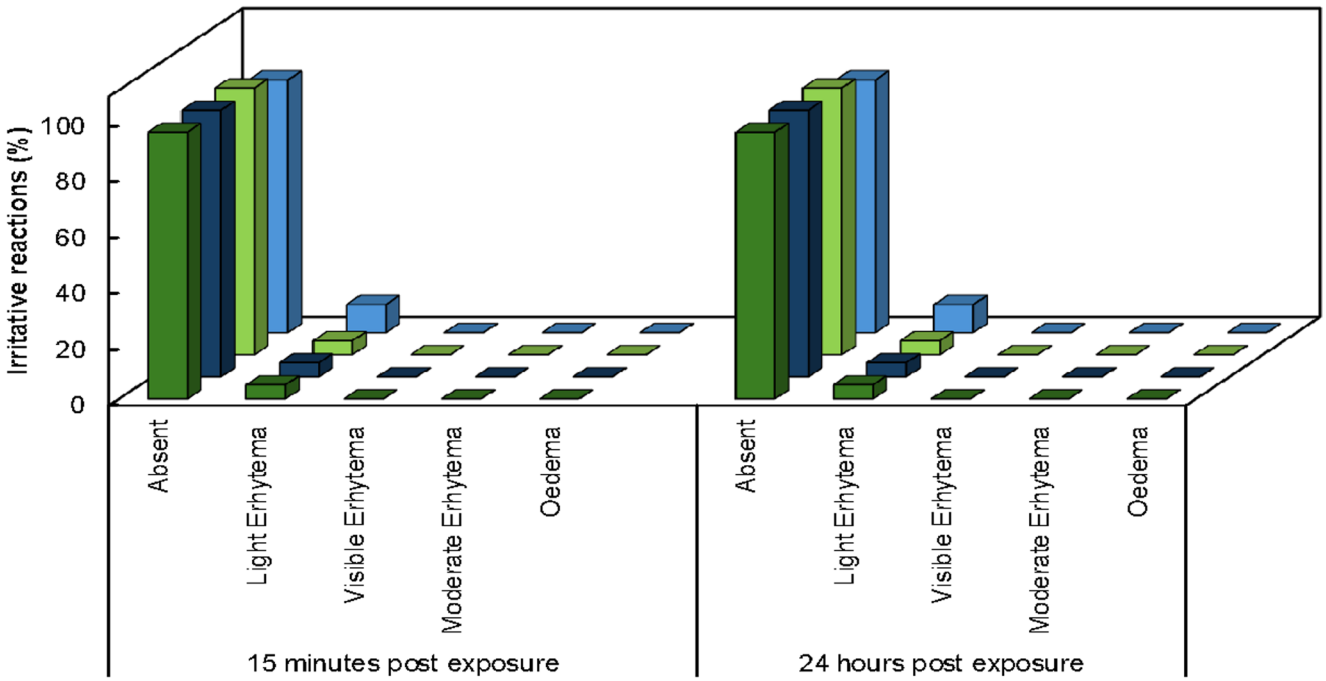

Fig. 6 In vivo irritative reactions on 20 healthy volunteers acquired by patch test of Cy/RU (green) and RUCyL (blue) dispersed in xanthan gum (dark color) or carbopol (light color)

Korsmeyer-Peppas equation fitting, confirm that the mechanism of drug transport is diffusion-controlled indicating that the drug exhibits a fickian diffusion in all formulations, according to the type of delivery system. In details, concerning n values of Cy complexes, they are all around 0.5, slightly higher when viscosized, in accordance with literature findings [20, 43]. This result indicates that the drug release depends on the concentration gradient, and it is related to the time it takes to exit the internal Cy cavity. The presence of XG and CRP does not affect the release mechanism of RU from the Cy complex, but it optimizes the viscosity in the semisolid form for skin application. The same statement can be described for liposomes formulations. All n exponents are lower than 0.43, that represents the reference value of fickian limit for spherical geometry such as liposomes [44, 45], confirming that the drug follows a fickian diffusion. Also in this case, the increase in viscosity obtained by XG or CRP preserves the diffusion mechanism of RU, improving the technological formulation and patient compliance.

In Vivo Patch Test

A patch test was performed to evaluate the safety of the produced Cy/RU and RUCyL formulations for potential administration onto the skin. Precisely, the potential irritation caused by applying the formulation onto the skin has been evaluated on 20 healthy volunteers and the results expressed as a percentage of irritative reactions (Fig. 6). It was found that both the gel preparations after 48 h of application under occlusive conditions can be classified as non-irritant and, therefore, are considered safe. Based on the results, both gel preparations can be classified as non-irritant after 48 h of application under occlusive conditions and so considered safe. The suitability of these systems for topical application was confirmed by the absence of irritative reactions in 95% of cases and negligible reactions in the remaining 5%.

Conclusion

This research study enabled the design and characterization of RU-loaded supramolecular nanosystems based on the use of Cy complexes formulated alone or included in liposomes (CyL). From the comparison of the performances of the two different supramolecular systems, it was found that both formulations maintain their physico-chemical stability in terms of color, size, rutin content, and antioxidant activity over time. However, the antioxidant assays demonstrated a greater activity when rutin is encapsulated within CyL. Comparative in vitro studies on drug diffusion suggested an improved delivery of RU, possibly controlled by the vesicular system; in contrast, the increase in viscosity of the formulations obtained by the addition CRP or XG showed a lower spreadability and greater adhesiveness, ensuring effective skin application. On the other hand, the patch tests demonstrated an optimal tolerance by the skin of both formulations. Based on these results, the produced Cy/

RU and RUCyL formulations may represent an interesting starting point for the topical application of natural antioxidant molecules.

In summary, the dual encapsulation of rutin through cyclodextrin complexation and liposomal delivery, combined with gelation, offers a synergistic approach that enhances topical release and antioxidant efficacy. This strategy addresses the limitations of RU solubility and stability, ensuring improved skin retention and controlled release, and represents a promising platform for the development of advanced dermal formulations. The main difference between the RUCyL here proposed and previously published rutin-loaded liposomes or cyclodextrin gels lies in the higher encapsulation efficiency and improved stability of the carried drug as compared to the other systems. For topical skin application, the use of RUCyL systems combines the advantages of increased stability of the encapsulated active ingredient with the lipid composition of the vesicle, which would allow for more efficient interaction with the stratum corneum, improving the treatment of dermatological conditions. This, as shown in the literature, is not always achieved with loading on sole liposomes or cyclodextrins [21, 46–49]. While the present manuscript represents a preliminary technological study focused on formulation development, future experiments will employ i*n vitro* (e.g., keratinocytes) and ex vivo models (e.g., skin explants) to better elucidate the behavior of the different formulations in terms of cutaneous permeability as well as their biological effects and modulation of pathways involved in cutaneous inflammation and antioxidant responses.

Acknowledgements The authors thanks Dr. Leda Montesi of the Cosmetology Center of the University of Ferrara for technical support and Dr. Ismaela Fracasso for technical issue. The Authors thank University of Ferrara FIRD2023, FAR2023 and FAR2024.

Author Contributions R.C. and M.S. conceptualized and wrote the original draft of the manuscript; R.C., S.M., M.S and F.F. made review and editing; M.S., M.D. and A.B. conducted the experiments; F.F. and A.B. data curation; M.S. and R.C. funding acquisition. All authors reviewed the manuscript.

Funding Open access funding provided by Università degli Studi di Ferrara within the CRUI-CARE Agreement.

Data Availability The datasets generated during and/or analyzed during the current study are available from the corresponding author on reasonable request.

Declarations

Ethics Approval and Consent to Participate The study was conducted in accordance with the Declaration of Helsinki and was approved by the Ethics Committee of the University of Ferrara, Italy (protocol code: 170583; date of approval: 16 November 2017).

Competing interests The authors declare no competing interests.

References

1. Esposito E, Nastruzzi C, Sguizzato M, Cortesi R. Nanomedicines to treat skin pathologies with natural molecules. CPD. 2019;25:2323–37. https://doi.org/10.2174/1381612825666190709210703.
2. Wong R, Geyer S, Weninger W, et al. The dynamic anatomy and patterning of skin. Exp Dermatol. 2016;25:92–8. https://doi.org/10.1111/exd.12832.
3. Ferrara F, Pambianchi E, Woodby B, et al. Evaluating the effect of ozone in UV induced skin damage. Toxicol Lett. 2021;338:40–50. https://doi.org/10.1016/j.toxlet.2020.11.023.
4. Vongelis P, Koulouris NG, Bakakos P, Rovina N. Air pollution and effects of tropospheric ozone (O3) on public health. Int J Environ Res Public Health. 2025;22:709. https://doi.org/10.3390/ijerph22050709.
5. Chinembiri T, Du Plessis L, Gerber M, et al. Review of natural compounds for potential skin cancer treatment. Molecules. 2014;19:11679–721. https://doi.org/10.3390/molecules190811679.
6. Ben Sghaier M, Pagano A, Mousslim M, et al. Rutin inhibits proliferation, attenuates superoxide production and decreases adhesion and migration of human cancerous cells. Biomed Pharmacother. 2016;84:1972–8. https://doi.org/10.1016/j.biopha.2016.11.001.
7. Corina D, Florina B, Iulia P, et al. Rutin and its cyclodextrin inclusion complexes: physico-chemical evaluation and in vitro activity on B164A5 murine melanoma cell line. CPB. 2018;18:1067–77. https://doi.org/10.2174/1389201019666180209165523.
8. Choi SJ, Lee S-N, Kim K, et al. Biological effects of rutin on skin aging. Int J Mol Med. 2016;38:357–63. https://doi.org/10.3892/ijmm.2016.2604.
9. Peres DA, De Oliveira CA, Da Costa MS, et al. Rutin increases critical wavelength of systems containing a single UV filter and with good skin compatibility. Skin Res Technol. 2016;22:325–33. https://doi.org/10.1111/srt.12265.
10. Kamel R, Mostafa DM. Rutin nanostructured lipid cosmeceutical preparation with sun protective potential. J Photochem Photobiol B. 2015;153:59–66. https://doi.org/10.1016/j.jphotobiol.2015.09.002.
11. Martins RM, De Siqueira Martins S, Barbosa GLF, et al. Photoprotective effect of solid lipid nanoparticles of rutin against UVB radiation damage on skin biopsies and tissue-engineered skin. J Microencapsul. 2022;39:668–79. https://doi.org/10.1080/02652048.2022.2156631.
12. Oliveira CAD, Peres DD, Graziola F, et al. Cutaneous biocompatible rutin-loaded gelatin-based nanoparticles increase the SPF

of the association of UVA and UVB filters. Eur J Pharm Sci. 2016;81:1–9. https://doi.org/10.1016/j.ejps.2015.09.016.
13. Tomazelli LC, De Assis Ramos MM, Sauce R, et al. SPF enhancement provided by rutin in a multifunctional sunscreen. Int J Pharm. 2018;552:401–6. https://doi.org/10.1016/j.ijpharm.2018.10.015.
14. Li J, Ni W, Aisha M, et al. A rutin nanocrystal gel as an effective dermal delivery system for enhanced anti-photoaging application. Drug Dev Ind Pharm. 2021;47:429–39. https://doi.org/10.1080/03639045.2021.1890113.
15. Pinzaru I, Chioibas R, Marcovici I, et al. Rutin Exerts Cytotoxic and Senescence-Inducing Properties in Human Melanoma Cells. Toxics. 2021;9:226. https://doi.org/10.3390/toxics9090226.
16. Hassan AS, Soliman GM. Rutin Nanocrystals with Enhanced Anti-Inflammatory Activity: Preparation and Ex Vivo/In Vivo Evaluation in an Inflammatory Rat Model. Pharmaceutics. 2022;14:2727. https://doi.org/10.3390/pharmaceutics14122727.
17. Saha R, Patkar S, Pillai MM, Tayalia P. Bilayered skin substitute incorporating rutin nanoparticles for antioxidant, anti-inflammatory, and anti-fibrotic effect. Biomaterials Advances. 2023;150:213432. https://doi.org/10.1016/j.bioadv.2023.213432.
18. Dewangan HK, Shah K, Vadaga AK, et al. Optimisation and evaluation of long circulating Ru-SLNs carrier for targeting melanoma cells. J Microencapsul. 2025;42:107–19. https://doi.org/10.1080/02652048.2024.2443436.
19. Pinzaru I, Tanase A, Enatescu V, et al. Proniosomal gel for topical delivery of rutin: preparation, physicochemical characterization and in vitro toxicological profile using 3D reconstructed human epidermis tissue and 2D cells. Antioxidants. 2021;10:85. https://doi.org/10.3390/antiox10010085.
20. Naeem A, Yu C, Zang Z, et al. Synthesis and evaluation of rutin–hydroxypropyl β-cyclodextrin inclusion complexes embedded in xanthan gum-based (HPMC-g-AMPS) hydrogels for oral controlled drug delivery. Antioxidants. 2023;12:552. https://doi.org/10.3390/antiox12030552.
21. Sguizzato M, Ferrara F, Sisto M, et al. Rutin-containing cyclodextrin nanosystems: a possible strategy for dietary supplementation in diabetics. J Drug Deliv Sci Technol. 2025;110:107065. https://doi.org/10.1016/j.jddst.2025.107065.
22. Sguizzato M, Ferrara F, Drechsler M, et al. Lipid-based nanosystems for the topical application of Ferulic acid: a comparative study. Pharmaceutics. 2023;15:1940. https://doi.org/10.3390/pharmaceutics15071940.
23. Pattni BS, Chupin VV, Torchilin VP. New developments in liposomal drug delivery. Chem Rev. 2015;115:10938–66. https://doi.org/10.1021/acs.chemrev.5b00046.
24. Pecora R. Dynamic light scattering measurement of nanometer particles in liquids. J Nanopart Res. 2000;2:123–31. https://doi.org/10.1023/A:1010067107182.
25. Danaei M, Dehghankhold M, Ataei S, et al. Impact of particle size and polydispersity index on the clinical applications of lipidic nanocarrier systems. Pharmaceutics. 2018;10:57. https://doi.org/10.3390/pharmaceutics10020057.
26. Sguizzato M, Agosta F, Ciancetta A, et al. Supramolecular delivery systems for polyphenols: a green approach to predict *in vivo* permeability through an *in vitro* setup. Int J Pharm. 2025;670:125170. https://doi.org/10.1016/j.ijpharm.2025.125170.
27. Andrade LM, de Fátima Reis C, Maione-Silva L, et al. Impact of lipid dynamic behavior on physical stability, in vitro release and skin permeation of genistein-loaded lipid nanoparticles. Eur J Pharm Biopharm. 2014;88:40–7. https://doi.org/10.1016/j.ejpb.2014.04.015.
28. Blois MS. Antioxidant determinations by the use of a stable free radical. Nature. 1958;181:1199–200. https://doi.org/10.1038/1811199a0.
29. Wang M, Li J, Rangarajan M, et al. Antioxidative phenolic compounds from sage (*Salvia officinalis*). J Agric Food Chem. 1998;46:4869–73. https://doi.org/10.1021/jf980614b.
30. Benzie IFF, Strain JJ. The ferric reducing ability of plasma (FRAP) as a measure of antioxidant power: the FRAP assay. Anal Biochem. 1996;239:70–6. https://doi.org/10.1006/abio.1996.0292.
31. Esposito E, Sguizzato M, Bories C, et al. Production and characterization of a clotrimazole liposphere gel for candidiasis treatment. Polymers. 2018;10:160. https://doi.org/10.3390/polym10020160.
32. Esposito E, Drechsler M, Mariani P, et al. Nanostructured lipid dispersions for topical administration of crocin, a potent antioxidant from saffron (*Crocus sativus* L.). Materials Science and Engineering: C. 2017;71:669–77. https://doi.org/10.1016/j.msec.2016.10.045.
33. Nohynek GJ, Antignac E, Re T, Toutain H. Safety assessment of personal care products/cosmetics and their ingredients. Toxicol Appl Pharmcol. 2010;243:239–59. https://doi.org/10.1016/j.taap.2009.12.001.
34. Robinson MK, Cohen C, de Fraissinette A de B, et al. Non-animal testing strategies for assessment of the skin corrosion and skin irritation potential of ingredients and finished products. Food Chem Toxicol. 2002;40:573–92. https://doi.org/10.1016/S0278-6915(02)00005-4.
35. SCCNFP/0245/99. Opinion concerning Basic Criteria of the protocols for the skin compatibility testing of potentially cutaneous irritant cosmetic ingredients or mixtures of ingredients on human volunteers, adopted by the SCCNFP during the plenary session of 8 December 1999.
36. Nguyen TA, Liu B, Zhao J, et al. An investigation into the supramolecular structure, solubility, stability and antioxidant activity of rutin/cyclodextrin inclusion complex. Food Chem. 2013;136:186–92. https://doi.org/10.1016/j.foodchem.2012.07.104.
37. Wangsawangrung N, Choipang C, Chaiarwut S, et al. Quercetin/Hydroxypropyl-β-cyclodextrin inclusion complex-loaded hydrogels for accelerated wound healing. Gels. 2022;8:573. https://doi.org/10.3390/gels8090573.
38. Cristiano MC, Barone A, Mancuso A, et al. Rutin-loaded nanovesicles for improved stability and enhanced topical efficacy of natural compound. JFB. 2021;12:74. https://doi.org/10.3390/jfb12040074.
39. Halevas EG, Avgoulas DI, Katsipis G, Pantazaki AA. Flavonoid-liposomes formulations: physico-chemical characteristics, biological activities and therapeutic applications. European Journal of Medicinal Chemistry Reports. 2022;5:100059. https://doi.org/10.1016/j.ejmcr.2022.100059.
40. Park SN, Lee MH, Kim SJ, Yu ER. Preparation of quercetin and rutin-loaded ceramide liposomes and drug-releasing effect in liposome-in-hydrogel complex system. Biochem Biophys Res Commun. 2013;435:361–6. https://doi.org/10.1016/j.bbrc.2013.04.093.
41. Cândido TM, De Oliveira CA, Ariede MB, et al. Safety and antioxidant efficacy profiles of rutin-loaded ethosomes for topical application. AAPS PharmSciTech. 2018;19:1773–80. https://doi.org/10.1208/s12249-018-0994-3.
42. Jin F, Cao M, Zhang H, et al. Preparation of zein-rutin supramolecular nanoparticles using pH-ultrasound-shifting: binding mechanism, functional properties, and in vitro release kinetics. Food Chem. 2025;483:144087. https://doi.org/10.1016/j.foodchem.2025.144087.
43. Pyrak B, Rogacka-Pyrak K, Gubica T, Szeleszczuk Ł. Exploring cyclodextrin-based nanosponges as drug delivery systems: understanding the physicochemical factors influencing drug loading

and release kinetics. IJMS. 2024;25:3527. https://doi.org/10.3390/ijms25063527.
44. Wu IY, Bala S, Škalko-Basnet N, Di Cagno MP. Interpreting non-linear drug diffusion data: utilizing Korsmeyer-Peppas model to study drug release from liposomes. Eur J Pharm Sci. 2019;138:105026. https://doi.org/10.1016/j.ejps.2019.105026.
45. Gil-Gonzalo R, Durante-Salmerón DA, Pouri S, et al. Chitosan-coated liposome formulations for encapsulation of ciprofloxacin and etoposide. Pharmaceutics. 2024;16:1036. https://doi.org/10.3390/pharmaceutics16081036.
46. Maleki Dizaj S, Tohidi S, Salatin S, et al. Antibacterial potential of rutin nanoformulations: current insights and future directions. Biomed Pharmacother. 2026;195:118980. https://doi.org/10.1016/j.biopha.2026.118980.
47. Wang W-X, Feng S-S, Zheng C-H. A comparison between conventional liposome and drug-cyclodextrin complex in liposome system. Int J Pharm. 2016;513:387–92. https://doi.org/10.1016/j.ijpharm.2016.09.043.
48. Almeleebia TM, Goyal N, Akhter MH, et al. β-cyclodextrin/PVP-stabilized nanocrystal gel for dual release of rutin and thymoquinone for wound healing. J Clust Sci. 2025;36:13. https://doi.org/10.1007/s10876-024-02735-5.
49. Aldawsari MF, Alam A, Imran M. Rutin-loaded transethosomal gel for topical application: a comprehensive analysis of skin permeation and antimicrobial efficacy. ACS Omega. 2024;9:27300–11. https://doi.org/10.1021/acsomega.4c01718.